



RESEARCH ON THE CLASSIFICATION FOR FAULTS OF ROLLING BEARING BASED ON MULTI-WEIGHTS NEURAL NETWORK

Yujian Qiang¹, Ling Chen¹, Liang Hua*¹, Juping Gu¹, Lijun Ding², Yuqing Liu¹

¹College of Electrical Engineering, Nantong University, Nantong, 226019, China

²College of Electro-mechanics Engineering, Jiaxing University, Jiaxing, 310032, China

Emails: ntdxhualiang@163.com

Submitted: Mar. 15, 2014

Accepted: June 30, 2014

Published: Sep. 1, 2014

Abstract- A methodology based on multi-weights neural network (MWNN) is presented to identify faults of rolling bearing. With considerations of difficulties in analyzing rolling bearing vibration data, we analyzed how to extract time domain feature parameters of faults. Further, the time domain feature parameters extracted from fault signals are utilized to train multi-weights neural network for achieving an optimal coverage of fault feature space. Thus, faults of rolling bearing can be identified. Finally, simulation results based on real sampling data indicate the effectiveness of the methodology proposed in this paper. In addition, simulation results also indicate that MWNN utilized in this paper is more excellent than probabilistic neural network (PNN) and suitable for the classification of small samples.

Index term: time domain parameter, multi-weights neural network, probabilistic neural network (PNN) algorithm, bearing fault classification.

I. INTRODUCTION

Rotating machineries are widely utilized in modern industrial systems, such as, steam turbines, compression machines, fans, mills, et al. Failure probabilities of these machineries are far larger than those of other machineries due to harsh working environments, long operation periods and frequent start-stop operations. Moreover, faults of rotating machineries may lead to chain reactions which may cause breakdown of whole systems [1]. In certain serious conditions, disastrous accidents that cause deaths and major economic losses may take place as a result of a small fault of the rotation machine. As a result, identification of potential or existing faults of rotating machineries is a key approach to guarantee safe operations. Theoretical methods and technical strategies of mechanical faults under different conditions and running states are the ways to guarantee stable operations of rotating machineries [2-5].

Rotating machineries are currently developed in directions of precision, automation and complication. Under this condition, probabilities and types of rotating machinery failures are consequently increased. Therefore, traditional methodology for mechanical fault diagnosis based on personal experience is out of date. Signal analysis and processing is widely applied in extracting useful symptoms from fault diagnosis. Fourier analysis and corresponding FFT algorithm are initial methodologies to analyze fault signals. FFT algorithm can realize various signal analysis such as spectrum analysis, correlation analysis [6], time series analysis [7], and cepstrum analysis [8], etc, and plays an important role in fault diagnosis procedure. However, Fourier analysis is only suitable for continuous, smooth time-domain signals. Nowadays, other methods based on perspective of frequency domain, including wavelet analysis [9], Hilbert spectrum [10] and instantaneous frequency estimation [11] have been successfully utilized in this area.

Precise mathematical models, effective state estimations, parameter estimations, and appropriate statistical decision methods are basis of traditional motor fault diagnosis methodologies. Unfortunately, these factors are difficult to obtain and consequently bring considerable limitations

to traditional motor fault diagnosis [12-13]. For overcoming this shortcoming, big varieties of artificial intelligence algorithms such as neural network, fuzzy logic, fuzzy neural control and genetic algorithm, et al, have been utilized in the area of motor fault diagnosis. Compared with traditional methodologies, these artificial intelligence algorithms have excellent performances on speech recognition, face recognition and some other fields. These algorithms are regarded as important trends of motor diagnosis technology.

In traditional methodology, optimal partition of different types of samples in the space is a goal of recognition. The most typical methodology is support vector machine (SVM) theory, but it turns out to be ineffective in practical application, which can be explained from two aspects. From the view of mathematical models, since traditional recognition modes are based on Bayesian statistics theory and the convergence condition is decided by empirical risk minimization principle, the result of classification won't be obvious unless the classification decision is made through a large number of samples. Besides, the estimation of probability density function becomes more difficult along with massive increase of samples. Therefore, accurate probability statistical methods based on mathematical statistics cannot completely apply to the pattern recognition. However, the bionic pattern recognition based on multi-weights neural network is aimed at an optimum coverage of the same type of samples' distribution in a specific space. In another words, the structure of every type of sample subspace relies only on the sample type itself, which is totally different from the way to establish subspace relying on the relationships between various sample types in traditional pattern recognition. When constructing the subspace of a certain sample, bionic pattern recognition adopts complex geometrical objects to cover space by analyzing the relationship between the same types of training samples [14]. Multi-weights neural network has been widely used in various areas such as face identification, voice identification, and medical image analysis, etc. In this paper, it is applied to the classification of rolling bearing faults, which also turns out to be effective.

In this paper, the time-domain analysis method is adopted for rotating bearing faults recognition, which is the earliest method in fault diagnosis and is still popular with the majority of researchers.

Diagnosis is carried out by analyzing feature parameters of vibration signals. These feature parameters can be divided into two categories, i.e., dimension parameters and dimensionless parameters. Dimension parameters include mean, root-mean-square (RMS) value, and variance. Dimensionless parameters comprise waveform index, peak index, pulse index, square amplitude, margin index, and kurtosis index. Generally speaking, these feature parameters are unrelated to size, load, and speed changes of rolling bearings, but determined by the extent and type of bearing faults. The extracted time-domain feature parameters are sent to train multi-weights neural network which constructed by the training set of bearing faults in order to identify rolling bearing faults. The experimental results verified that MWNN is not only more excellent than PNN algorithm, but also more suitable for the classification of small samples.

II. FAULT FEATURE EXTRACTION METHOD

Regarding vibration signals, a base of signal processing is how to extract characteristic parameters of those signals. There are so many existed methodologies that can be utilized for bearing fault extraction, such as wavelet packet analysis based on time-domain, local mean decomposition based on time-frequency analysis, et al. In this paper, we analyze essential features of vibration signals from time-domain aspect. The mean value reflects the amount of vibration energy, if exceptions occur in the bearing, vibration energy will increase subsequently. The peak factor is used to diagnose bearing fault because its value is not affected by the bearing size, speed or load. Under normal condition, the value of peak factor is approximately 5, however, it will arrive at tens in conditions of failure. Furthermore, kurtosis index is sensitive to impulsion feature in signal, and its value is around 3 normally. If the value of kurtosis index approaches 4 or even exceeds 4, it means there is impulsive vibration in operating machine.

In preliminary stage of faults, changes of effective value are tiny, but changes of kurtosis index are remarkable at the same time, it can increase from 3 to tens even more than one hundred. That is to say, the changes of kurtosis index can provide early prediction of faults. Therefore, we

regard time-domain parameters as the classification feature to recognize faults. The formulas of time-domain feature parameters in this paper are given below, including maximum, RMS, mean, variance, waveform index, peak index, pulse index, square amplitude, margin index, and kurtosis index. In the following formula, X refers to n dimensional vector, which represents a sample of one rolling bearing fault's vibration signal.

$$\text{Maximum: } X_{\max} = \max \{ |x_i| \}, i = 1, 2, \dots, N$$

$$\text{RMS: } X_{rms} = \sqrt{\frac{1}{N} \sum_{i=1}^N x_i^2}, i = 1, 2, \dots, N$$

$$\text{Mean: } \bar{X} = \frac{\sum_{i=1}^N x_i}{N}, i = 1, 2, \dots, N$$

$$\text{Variance: } S^2 = \frac{1}{N} \sum_{i=1}^N (x_i - \bar{X})^2, i = 1, 2, \dots, N$$

$$\text{Waveform index: } S_f = \frac{X_{rms}}{|\bar{X}|}$$

$$\text{Pulse index: } I_f = \frac{X_{\max}}{|\bar{X}|}$$

$$\text{Peak index: } C_f = \frac{X_{\max}}{X_{rms}}$$

$$\text{Square amplitude: } X_r = \left(\frac{1}{N} \sqrt{|x_i|} \right)^2, i = 1, 2, \dots, N$$

$$\text{Margin index: } CL_f = \frac{X_{\max}}{X_r}$$

$$\text{Kurtosis index: } K_v = \frac{\frac{1}{N} \sum_{i=1}^N x_i^4}{X_{rms}^4}, i = 1, 2, \dots, N$$

III. DESCRIPTION OF MULTI-WEIGHTS NEURON NETWORK

Compared with conventional pattern recognition methods, the meaning of bio-mimetic pattern recognition is that all useful information is contained in training set. This methodology is based

on "understanding" rather than "difference" [15]. Without the support of prior knowledge, samples in the training set explore optimal classification by obtaining an optimal coverage of the same type's samples in the feature space. The key is to introduce the recognition principle "body covered non-sphere complex geometry in multi-dimensional space" which built according to certain universal regularities among the same kind of samples. Such continuous regularities are objective truths conformed to human intuitive understanding. Objects of the same kind in the feature spaces are continuous, and things within the same continuity interval are organized in the same category. By this way, it is conducive to the improvement of people's understanding towards different things.

In the bio-mimetic pattern recognition, MWNN can be considered as a closed hyper-surface in high-dimensional space. All the samples of one kind lying in one irregular connected region need to be established a complex geometry to cover this region in a high-dimensional space. Different kinds of samples construct different complex geometries. If the recognized samples lie in one certain closed region, they will be recognized correctly as the type, and vice versa. The schematic diagram of division in two-dimensional space is illustrated as figure 1.

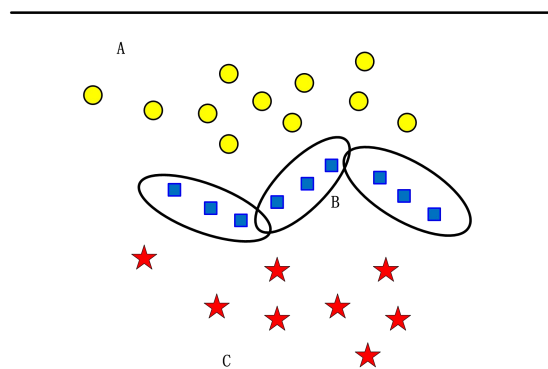


Figure 1. Schematic diagram of division in MWNN

A. Mathematical model

The multi-weights neural network utilized in bio-mimetic pattern recognition can cover the performances of both BP neural network and RBF neural network. It can realize various closed

hyper-surface characteristics. Shapes of hyper-surfaces can be changed along with the number of weight. Hyper-surfaces can be stretched or compressed in different directions. Some operations can be conducted by changing a few parameters according to the practical demands. As is shown in this article, neural network has become an appropriate method as well as a practical tool for the construction of high dimensional spatial data sets.

Thus, a basic model of universal neurons is established as Eq. (1.1) [15].

$$Y = f \left[\sum_{i=1}^n \varphi(w_i, w'_i, w''_i, \dots, x_i) - \theta \right] \quad (1.1)$$

Where $W = [w_1, w_2, \dots, w_n]$, $W' = [w'_1, w'_2, \dots, w'_n]$, and $W'' = [w''_1, w''_2, \dots, w''_n], \dots$ represent multi-weights vectors; $X = [x_1, x_2, \dots, x_n]$ is the input vector. This model describes the relationships amongst several input vectors and weights vectors. Therefore it can be called multi-weights vector neuron model, which can be presented as Eq. (1.2).

$$Y = f \left[\sum_{i=1}^n \varphi(w_i, w'_i, \dots, x_i) - \theta \right] \quad (1.2)$$

It can be seen as $Y = F$ (It represents the distance from X to the hyper-surface β), and the equation of hyper-surface β is described as Eq.(1.3).

$$\left[\sum_{i=1}^n \varphi(w_i, w'_i, \dots, x_i) - \theta \right] = 0 \quad (1.3)$$

When $n = 3$, it is named as the three-weights neuron, denoted here as $pSi3$ and expressed as Eq. (1.4).

$$\begin{cases} Y = f[\varphi(w_1, w_2, w_3, x) - \theta] \\ \varphi(w_1, w_2, w_3, x) = \|X - \psi_{(w_1, w_2, w_3)}\| \\ \psi_{(w_1, w_2, w_3)} = \{Y | Y = \alpha_2 [\alpha_1 W_1 + (1 - \alpha_1) W_2] + (1 - \alpha_2) W_3 \} \end{cases} \quad (1.4)$$

Where $\alpha_1 \in [0, 1]$, $\alpha_2 \in [0, 1]$, and $\psi_{(w_1, w_2, w_3)}$ represents a triangle constructed points W_1 , W_2 and W_3 . Then $\varphi(w_1, w_2, w_3, x) - \theta \leq 0$ describes a coverage that is determined by the topological product of $\psi_{(w_1, w_2, w_3)}$ and the hyper-sphere (radius is θ).

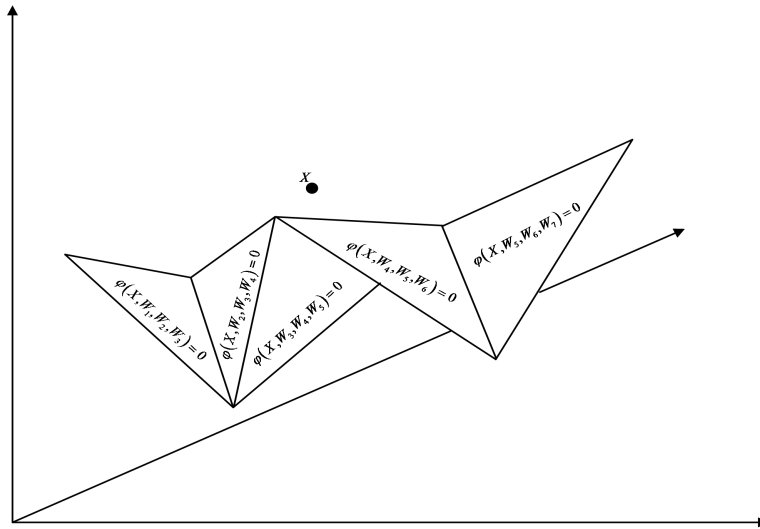


Figure 2. Illustration on geometrical mean of Multi-weights neuron networks^[14]

In figure 2, each neuron has 3 weights, and the network is a function of certain defined 'distance' between input point X and the 2-dimensional manifold consisted with triangles [14].

B. Steps of MWNN construction

It is Supposed that certain training sample set extracted from a specific type of fault is $X = \{X_1, X_2, \dots, X_N\}$, where N is the total number of sample points. $X_i = (x_1^i, x_2^i, \dots, x_m^i)$ is sample i in the sample set described above, where m means the dimensions of sample points, and $\rho_{X\psi_i}$ represents the Euclidean distance from X to ψ_i . $\alpha_1 \in [0,1]$, $\alpha_2 \in [0,1]$. The procedures of multi-weights neural network construction are given as follows:

Step 1: Calculations of Euclidean distances between every two points within the training sample set X , and denoted two points the Euclidean distance of them is the minimum as P_{11} and P_{12} . Among the rest of the points within sample set X , we should find a point to which the sum of distance from P_{11} and P_{12} is the shortest and is non-collinear with these two points, and denote this point as P_{13} . These three points can construct a closed region $\Delta P_{11}P_{12}P_{13}$, denoted here as ψ_1 .

A neuron $pSi3$ is applied to cover this region, and the coverage is:

$$P_1 = \{X \mid \rho_{X\psi_1} \leq \theta, X \in R^n\} \quad (1.5)$$

$$\psi_1 = \{Y \mid Y = \alpha_2 [\alpha_1 P_{11} + (1 - \alpha_1) P_{12}] + (1 - \alpha_2) P_{13}\} \quad (1.6)$$

Step 2: It is judged that whether the reset of points are covered by the geometry P_1 constructed in the previous step. Every point should be eliminated if it lies within the coverage of geometry. Among the points lying out of the geometry, we should find a point to which the sum of distance from P_{11} , P_{12} , and P_{13} is the shortest according to step 1, and mark it as point P_{21} . Besides, we calculate the Euclidean distances from P_{11} to P_{21} , P_{12} to P_{21} , and P_{13} to P_{21} respectively to facilitate description, then choose two of them with smaller and smallest values and mark them as P_{22} and P_{23} . Thus, P_{21} , P_{22} and P_{23} make up the second closed region $\Delta P_{21}P_{22}P_{23}$, which is marked as ψ_2 . Therefore, if we cover this region with another neuron $pSi3$, its coverage is:

$$P_2 = \{X \mid \rho_{X\psi_2} \leq \theta, X \in R^n\} \quad (1.7)$$

$$\psi_2 = \{Y \mid Y = \alpha_2 [\alpha_1 P_{21} + (1 - \alpha_1) P_{22}] + (1 - \alpha_2) P_{23}\} \quad (1.8)$$

Where $\rho_{X\psi_2}$ represents the distance between point X and closed region ψ_2 .

Step 3: We should eliminate all the points lying in the coverage of region P_{i-1} before calculating the minimum value of the sum of Euclidean distance from each of the rest of points to the group of three points that make up ψ_{i-1} . And we mark this point as P_{i1} . Similarly, we calculate the Euclidean distance from P_{i1} to the points that make up ψ_{i-1} , choose two of the points with smaller and smallest values and mark them as P_{i2} and P_{i3} . Points P_{i1} , P_{i2} and P_{i3} make up the i^{th} closed region $\Delta P_{i1}P_{i2}P_{i3}$ which is marked as ψ_i . If we cover this region with a new neuron $pSi3$, its coverage is:

$$P_i = \{X \mid \rho_{X\psi_i} \leq \theta, X \in R^n\} \quad (1.9)$$

$$\psi_i = \{Y | Y = \alpha_2 [\alpha_1 P_{i1} + (1 - \alpha_1) P_{i2}] + (1 - \alpha_2) P_{i3}\} \quad (1.10)$$

Step 4: Repeat the operations described in Step 3 until all the sample points are handled. Finally, we can construct M geometries. Given the complex of these geometries is marked as Ω .

$$\Omega = \bigcup_{j=1}^M \psi_j \quad (1.11)$$

C. Fault identification process of MWNN

We have obtained multi-weights neural network training sets that consist of time domain features of various fault signals. Namely, every type of training samples has got its own geometry complex in the feature space according to the training principle. We then will be able to do tests for fault classification using the training sets.

According to multi-weights neural network theory, we may know that the coverage area of every type of fault in the sample space is the union set of those neuron coverage areas:

$$\Omega = \bigcup_{j=1}^M \psi_j \quad (1.12)$$

Then we calculate the shortest distance ρ_i from sample Y to the i^{th} geometry complex Ω_i .

And ρ_i is defined as follows:

$$\rho_i = \min_{1 \leq j \leq M_i} \rho_{ij} \quad (1.13)$$

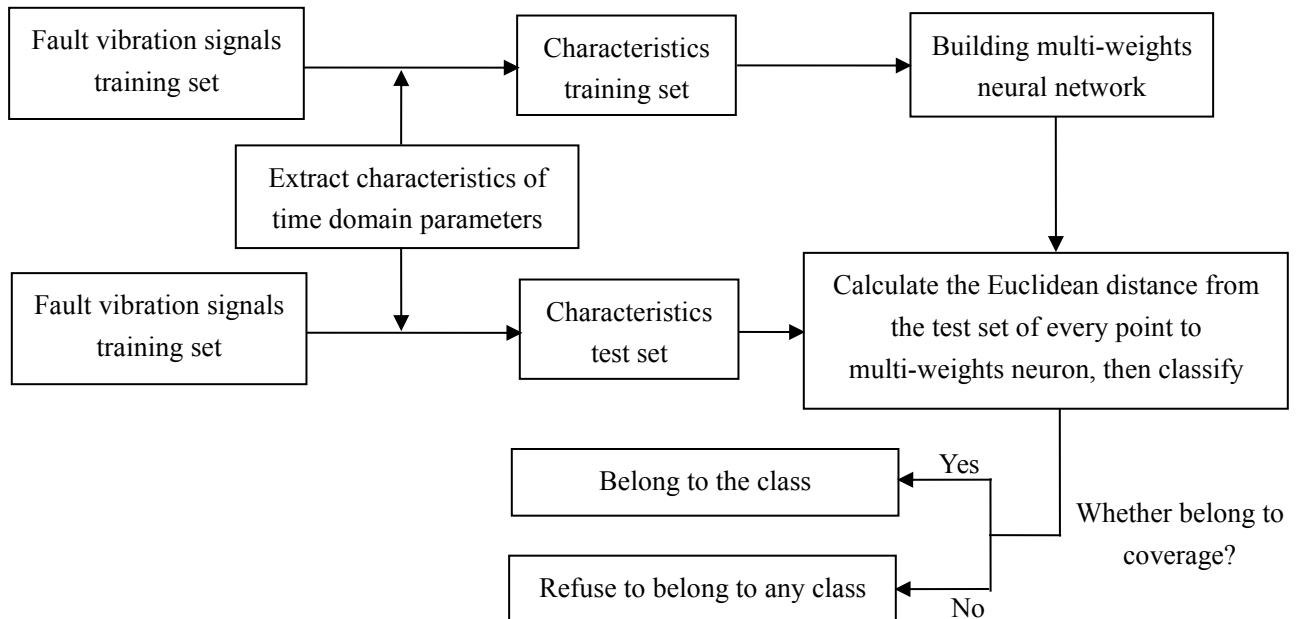


Figure 3. A flow chart about the identification of rolling bearing faults based on MWNN

Where ρ_{ij} is the distance between sample Y and the j^{th} geometry ψ_j of the i^{th} geometry complex Ω_i , and M_i means the number of geometries ψ_j within geometry complex Ω_i .

According to multi-weights neural algorithm, if the distance from sample Y to a type of geometry complex is the shortest, this type of fault includes sample Y .

So multi-weights neural recognition method achieves the classification of rolling bearing faults, and a flow chart about the identification of rolling bearing faults based on multi-weights neural network is shown in figure 3.

IV. EXPERIMENT

A. Bearing fault experimental introduction

In this paper, the bearing fault data comes from the bearing data center of Case Western Reserve University [16]. The experimental systems are illustrated as figure 4, in which a motor (on the left) is connected to automatic correction device, ergometer, torque transducer to drive the load (on the right) running. The test bearings support motor shaft rotation. Vibration data was collected by accelerometers, which were attached to the housing with magnetic bases. Accelerometers were placed at the 12 o'clock position at the drive end. Vibration signals were collected using a 16 channel DAT recorder, and were post processed in a Matlab environment. All data files are in Matlab (*.mat) format. Digital data was collected at 12,000 samples per second for drive end bearing faults.

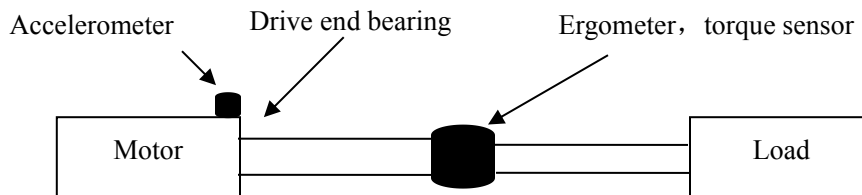


Figure 4. Experimental system

Outer races, inner races and rolling balls of three rolling bearings are artificially damaged by electrical discharge machining in this experiment. And time-domain vibration signals of normal operation, inner race fault, rolling ball fault and outer race fault are sampled.

B. Bearing Fault Classification

The paper selects 2 hp motor experiment data with the sample frequency 12Hz and motor speed 1750 rpm. We use ASUS X5DIJ computer to process vibration data. The computer's internal storage capacity is 2GB. The version of MATLAB is 7.8.0.347 (R2009a), 32-bit. Time-domain waveforms are shown in figure 5. As illustrated in the images, signals of inner race fault and outer race fault are too similar to distinguish.

In order to verify the efficiency of multi-weights neural network recognition method, four kinds of faults (normal operation, inner race fault, ball fault, and outer race fault) of rolling bearing are tested respectively in the experiment.

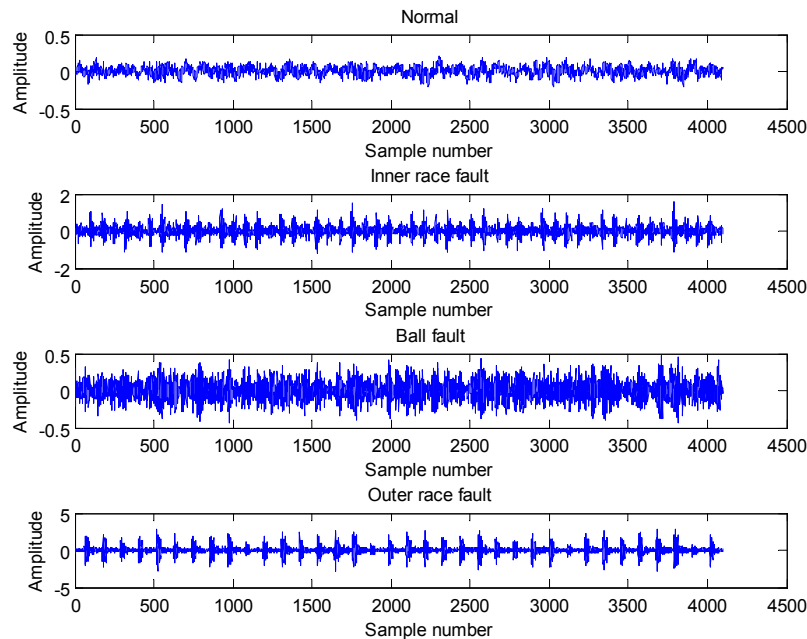


Figure 5. Time-domain waveform of sample fault data

Firstly, the ten time domain feature parameters are selected as the characteristic parameters of

fault signal to describe the rolling bearing fault categories. They are maximum, RMS, mean, variance, waveform index, peak index, pulse index, square amplitude, margin index, and kurtosis index.

In the recognition test, each type of fault signals is sampled by every 4096 points. Every sample contains points more than one period of signal. The training sets have 40 samples (every ten samples is a class), while the independent test sets also have 40 samples (every ten samples is a class). In order to verify the feasibility of data, as shown in Figure 6, we draw the distribution of data from the training sets in the first three principal components. The first three principal components are pulse index, maximum, and RMS. The effect of classification is still obvious when drawing the distribution of any other three main elements.

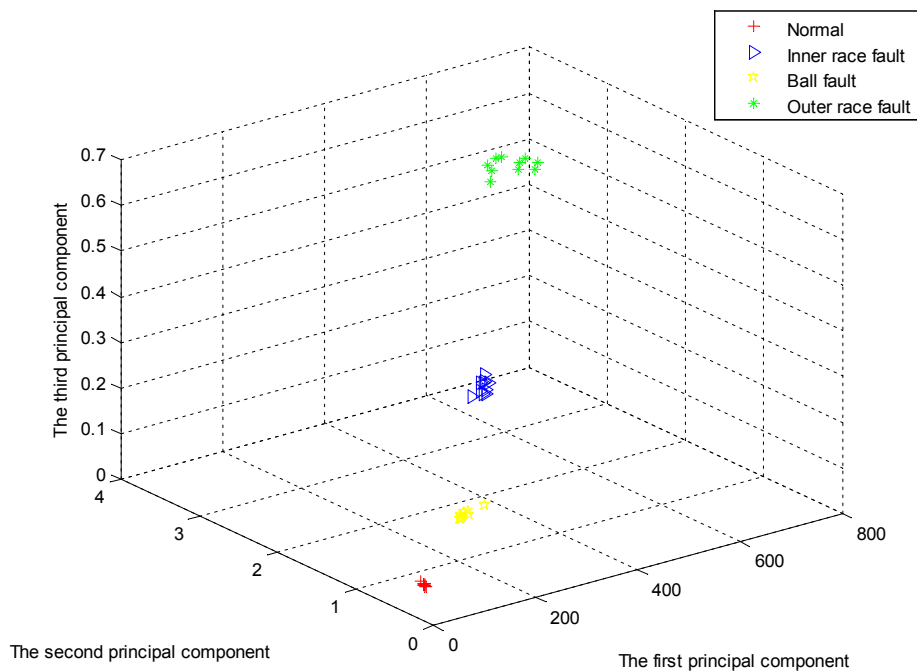


Figure 6. The distribution of the training set data in the first three principal components

In order to verify the stability and suitability of algorithms, we gradually reduce the number of each type of training samples. Each class reduces by 20% one time. It is illustrated in Table 1. Then, the original testing sets are also used for the following recognition. The result reveals that the recognition rate is 100%, when $Num = 10, 8, 6$.

Table 1: Training order and the corresponding number of each type of training samples

Training order	①	②	③	④	⑤
<i>Num</i>	10	8	6	4	3

By using MWNN algorithm, the shortest distance from the test samples to the training sets is fairly obvious. That is to say, the shortest sampling distance is crucial to judge the fault type. As shown in table 2, ρ_1 is the shortest among distances from ten normal samples to four types of fault multi-weight neuron ($\Omega_i (i=1,2,3,4)$, the training set) apparently. As is shown in figure 7, three of the samples which belong to the "ball fault" are mistakenly identified as "outer race faults" class when *Num* decreases to four and three. As a result, the corresponding recognition rate is 92.5%.

Table 2: ρ_i of 10 normal testing samples to $\Omega_i (i=1,2,3,4)$

Sample number	10 samples of each type of training				8 samples of each type of training				6 samples of each type of training			
	ρ_1	ρ_2	ρ_3	ρ_4	ρ_1	ρ_2	ρ_3	ρ_4	ρ_1	ρ_2	ρ_3	ρ_4
1	1.10	1.46	1.45	1.56	1.07	1.51	1.45	1.56	1.08	1.51	1.45	1.56
2	1.10	1.44	1.44	1.55	1.07	1.52	1.44	1.55	1.07	1.52	1.44	1.55
3	1.05	1.29	1.29	1.40	1.04	1.39	1.29	1.40	1.04	1.39	1.29	1.40
4	1.00	1.21	1.21	1.32	1.00	1.3	1.21	1.32	1.03	1.3	1.21	1.32
5	1.09	1.34	1.35	1.46	1.0	1.48	1.35	1.47	1.0	1.48	1.35	1.47
6	1.00	1.12	1.13	1.25	1.01	1.27	1.13	1.25	1.03	1.27	1.13	1.25
7	1.0	1.10	1.11	1.22	1.01	1.24	1.1	1.23	1.03	1.24	1.11	1.23
8	0.99	1.20	1.19	1.30	0.97	1.27	1.19	1.30	1.04	1.27	1.20	1.30
9	0.97	1.14	1.12	1.24	0.92	1.19	1.12	1.24	1.05	1.19	1.15	1.24
10	1.0	1.26	1.27	1.38	1.04	1.37	1.27	1.38	1.04	1.37	1.27	1.38

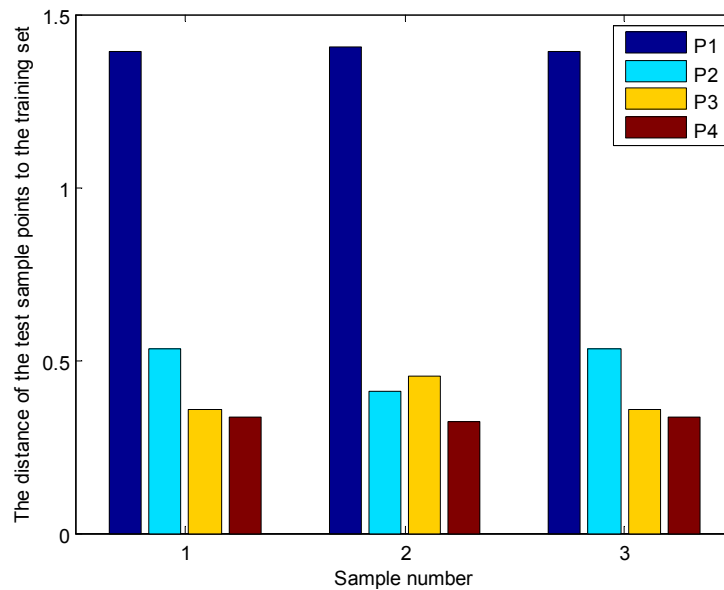


Figure 7. The minimum distance ρ_i from the three samples of the test set to Ω_i ($i=1,2,\dots,10$)

In this paper, the comparison between PNN algorithm and MWNN algorithm is made to obtain better classification effect. PNN proposed by Donald F. Specht in 1989 is a kind of mentor that learns feed forward neural networks. It uses least risk Bayesian rules for classification, and it has the advantage of parallel processing and classification estimation computing. PNN algorithm generally consists of the input layer, hidden layer, and output layer. Similarly, as is shown in Table 1, PNN algorithm uses the same samples of training sets and testing sets as MWNN. When $Num=10,8,6$, and the recognition rate of PNN is 90%, because four of the samples which originally belong to the "outer race fault" are mistakenly identified as "normal" class. When the sample number is four or three, the recognition rate of PNN is 82.5%, because seven of the samples which originally belong to the "outer race fault" are mistakenly identified as "normal" class. The results are given in Figure 8 and 9. As is illustrated in the figure, label "1" means "normal", label "2" means "inner race fault", label "3" means "ball fault", and label "4" means "outer race fault".

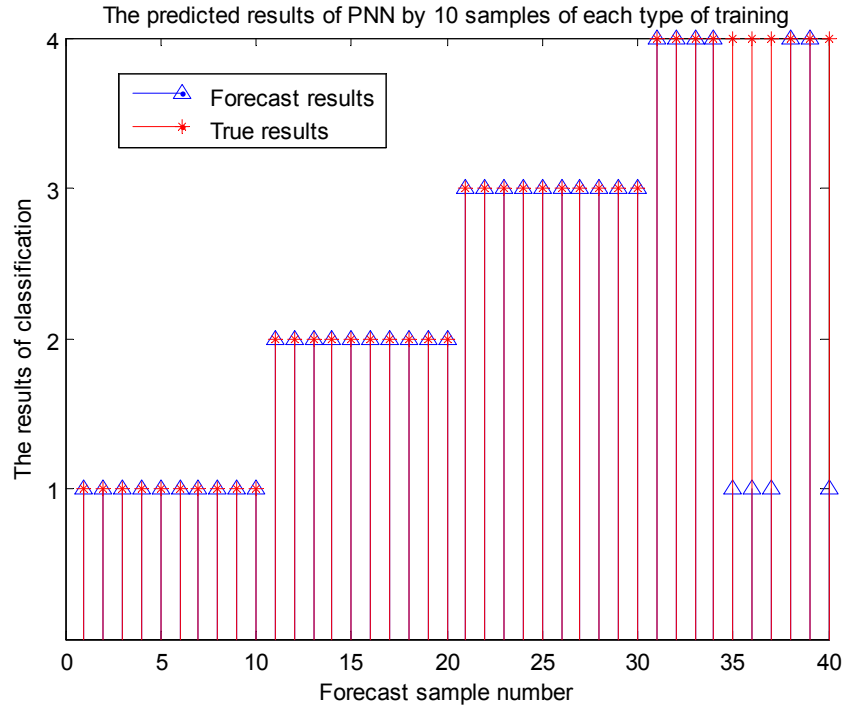


Figure 8. The predicted results of PNN by 10 samples of each type of training

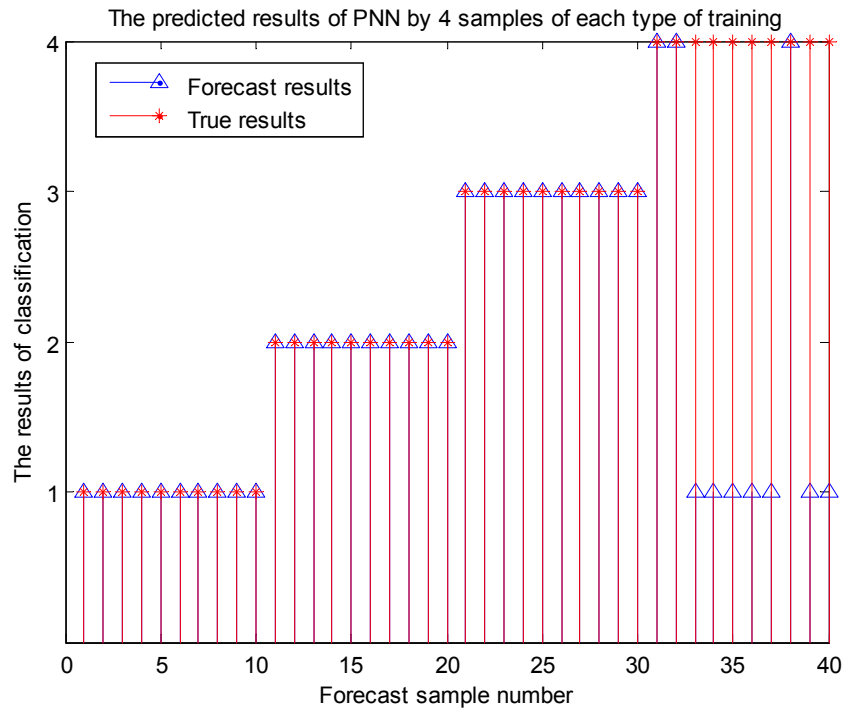


Figure 9. The predicted results of PNN by 4 samples of each type of training

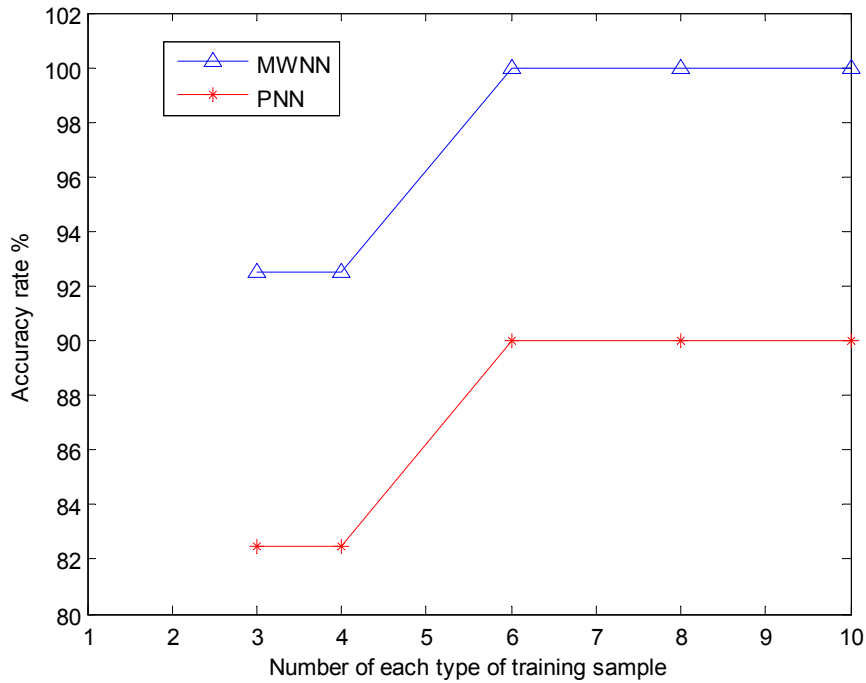


Figure 10. The compared result of MWNN and PNN

V. DISCUSSION

Through the comparison between two identification algorithms, figure 10 that shows the compared result of MWNN and PNN indicates that the method of MWNN for fault recognition is much better, because faults of the same kind in the feature spaces structured by the algorithm of MWNN are continuous, things within the same continuity interval are organized in the same category. MWNN algorithm aims to acquire optimal coverage of samples in the feature space. The shape of points from training sets constituted by one certain fault type will be analyzed and recognized in the high-dimensional space. Different types of samples construct different closed regions, namely different multi-weights neurons. After every type of faults' neuron is formed, we can send data from the testing sets to the multi-weights neural network for classification. Besides, the method of MWNN could set threshold θ_i for each class to prevent mistaken classification. Namely, if only the minimum distance ρ_i from testing sample X to Ω_i yield to the inequation $\rho_i \leq \theta_i$, that X would be classified to the i^{th} class; otherwise, it will be rejected to

recognize. However, PNN algorithm is easy to fall into local minima, which brings errors and reduces the accuracy of recognition.

VI. CONCLUSION

Multi-weights neural network algorithm applies point set topology as a mathematical analysis tool in the research of high- dimensional manifold. The purpose of the recognition algorithm is to acquire an optimal coverage of samples in the feature space. This paper has analyzed the bearing fault data in time-domain and extracted time-domain characteristic parameters as fault features. The MWNN algorithm improves the classification efficiency with short training time and high recognition accuracy. The experimental results illustrate that MWNN not only has more advantages than PNN algorithm, but also is more suitable for the classification of small samples.

ACKNOWLEDGMENTS

This work was supported by the National Natural Science Foundation of China (61273024 , 61305031), the Infrastructure Construction Foundation of Science and Technology in Jiangsu Province of China(BM2011089), Natural Science Fund for Colleges and Universities in Jiangsu Province(12KJB510023), and the Natural Science Foundation of Jiangsu Province (KB2012227).

REFERENCES

- [1] S. Zaidi, S. Aviyente, M. Salman, K. K. Shin, and E. Strangas, “Prognosis of gear failures in dc starter motors using hidden Markov models”, *IEEE Trans. Ind. Electron.* 2011, 58(5), pp. 1695-1706.
- [2] C. Chen, B. Zhang, G. Vachtsevanos, and M. Orchard, “Machine condition prediction based on adaptive neuro fuzzy and high-order particle filtering”, *IEEE Trans. Ind. Electron.*, 2011,

58(9), pp. 4353-4364.

[3] E. Strangas, S. Aviyente, J. Neely, and S. Zaidi, "Improving the reliability of electrical drives through failure prognosis", in Proc. IEEE SDEMPED, 2011, pp. 172-178.

[4] A. K. Mahamad, S. Saon, and T. Hiyama, "Predicting remaining useful life of rotating machinery based artificial neural network", Comput. Math. Appl. 2010, 60(4), pp. 1078-1087.

[5] T. Benkedjouh, K. Medjaher, N. Zerhouni, and S. Rechak, "Fault prognostic of bearings by using support vector data description", in Proc. IEEE PHM, 2012, pp. 1-7.

[6] Zhao Zhang, Mingbo Zhao, Chow, T.W.S, "Binary- and Multi-class Group Sparse Canonical Correlation Analysis for Feature Extraction and Classification", IEEE Transactions on Knowledge and Data Engineering, 2013, 25(10), pp: 2192-2205.

[7] Khatkhate, A., Ray, A., Keller, E., Gupta, S., Chin, S.C., "Symbolic time-series analysis for anomaly detection in mechanical systems", IEEE/ASME Transactions on Mechatronics, 2006, 11(4), pp: 439-447.

[8] Zhen Zhao, Fu-Li Wang, Ming-Xing Jia, Shu Wang, "Intermittent Chaos and Cepstrum Analysis Based Early Fault Detection on Shuttle Valve of Hydraulic Tube Tester", IEEE Transactions on Industrial Electronics, 2009, 56(7), pp: 2764-2770.

[9] Bezerra Costa, F, "Fault-Induced Transient Detection Based on Real-Time Analysis of the Wavelet Coefficient Energy", IEEE Transactions on Power Delivery. 2014, 29(1), pp.140-153.

[10] K Li, X.J. Chen, X Shi, etl, "Application of time frequency technology in failure diagnostics of shipborne antennas and drive system", Journal of Telemetry, Tracking and Command, 2011, 32(4), pp.33-40.

[11] Chun Ku Lee, Ki Seok Kwak, Tae Sung Yoon, Jin Bae Park, "Cable Fault Localization Using Instantaneous Frequency Estimation in Gaussian-Enveloped Linear Chirp Reflectometry", IEEE Transactions on Instrumentation and Measurement, 2013, 62(1), pp: 129 -139.

[12] Tommy W. S. Chow and Hong-Zhou Tan, "HOS-based non-parametric and parametric methodologies for machine fault detection", IEEE Trans. on Industrial Electronics, 2000, 47(5) :1051- 1059.

- [13] S.C.Mukhopadhyay, T.Ohji, M.Iwahara, S.Yamada and F.Matsumura, "A New Repulsion Type Magnetic Bearing - Modeling and Control", Proc. of the IEEE PEDS Conf, Singapore, pp 12-18, May 26-29, 1997.
- [14] Kral C., Wieser R. S. and Pirker F. , et al, "Sequences of field -oriented control for the detection of faulty rotor bars in induction machines- the Vienna Monitoring Method", IEEE Trans. On Industrial Electronics, 2000, 47(5) : 1042-1050.
- [15] Wang Shoujue, Liu Yangyang, Lai Jiangliang, Liu Xingxing, "Biomimetic pattern recognition and multi-weight neuron", National Defence Industry Press, Beijing, 2012.
- [16] T.Ohji, M.Kano, S.C.Mukhopadhyay, M.Iwahara and S.Yamada, "Characteristics of Rotating Vibration of Repulsive Type Magnetic Bearing Using Permanent Magnet", Journal of Magnetic Society of Japan, Vol. 24, No.4-2, pp. 1011-1014, 2000.
- [17] S.C.Mukhopadhyay, T.Ohji, M.Iwahara and S.Yamada, "Design, Analysis and Control of a New Repulsive Type Magnetic Bearing", IEE proceeding on Electric Power Applications, vol. 146, no. 1, pp. 33-40, January 1999.
- [18] T.Ohji, S.C.Mukhopadhyay, M.Iwahara and S.Yamada, "Permanent Magnet Bearings for Horizontal and Vertical Shaft Machines - A Comparative Study", Journal of Applied Physics, Vol. 85, No. 8, pp 4648-4650, April 1999.
- [19] Jianhui Hu, "Studies on Iris Recognition Algorithm Based on The Biomimetic Pattern Recognition", Zhejiang University of Technology, 2006.
- [20] M.Iwahara, S.C.Mukhopadhyay, S.Yamada and F.P.Dawson, "Development of Passive Fault Current Limiter in Parallel Biasing Mode", IEEE Transactions on Magnetics, Vol. 35, No. 5, pp 3523-3525, September 1999.
- [21] Case Western Reserve University Bearing Data center [EB/OL]. [http: // www.eecs.case.edu/laboratory/bearing](http://www.eecs.case.edu/laboratory/bearing).